SCIENTIFIC REPORTS

OPEN

SUBJECT AREAS:
DNA AND RNA
EXPERIMENTAL NUCLEAR PHYSICS
APPLIED PHYSICS
SENSORS AND BIOSENSORS

Received
30 January 2013

Accepted
7 June 2013

Published
24 June 2013

Correspondence and requests for materials should be addressed to V.M. (vkm49@skku.edu, vkm25749@gmail.com); T.K. (tkim@skku.edu) or S.H.P. (sunghapark@skku.edu)

* These authors contributed equally to this work.

A novel nanometric DNA thin film as a sensor for alpha radiation

Atul Kulkarni[1,2,3]*, Byeonghoon Kim[1,2]*, Sreekantha Reddy Dugasani[1,2]*, Pranav Joshirao[4], Jang Ah Kim[1,3], Chirag Vyas[4], Vijay Manchanda[4], Taesung Kim[1,3] & Sung Ha Park[1,2]

[1]Sungkyunkwan Advanced Institute of Nanotechnology (SAINT), Sungkyunkwan University, Suwon 440–746, Korea, [2]Department of Physics, Sungkyunkwan University, Suwon 440–746, Korea, [3]School of Mechanical Engineering, Sungkyunkwan University, Suwon 440–746, Korea, [4]Department of Energy Science, Sungkyunkwan University, Suwon 440–746, Korea.

The unexpected nuclear accidents have provided a challenge for scientists and engineers to develop sensitive detectors, especially for alpha radiation. Due to the high linear energy transfer value, sensors designed to detect such radiation require placement in close proximity to the radiation source. Here we report the morphological changes and optical responses of artificially designed DNA thin films in response to exposure to alpha radiation as observed by an atomic force microscope, a Raman and a reflectance spectroscopes. In addition, we discuss the feasibility of a DNA thin film as a radiation sensing material. The effect of alpha radiation exposure on the DNA thin film was evaluated as a function of distance from an ^{241}Am source and exposure time. Significant reflected intensity changes of the exposed DNA thin film suggest that a thin film made of biomolecules can be one of promising candidates for the development of online radiation sensors.

The Fukushima nuclear accident on March 2011 stressed the need for development of sensitive detectors in order to monitor the presence of alpha emitting radio nuclides as aerosols, dispersed particulate matter in the environment caused by fuel meltdown and overheating of discharged spent fuel[1–7]. Alpha particles, consisting of helium nuclei, are emitted by various isotopes of actinides including Th, U, Np, Pu, Am and Cm. These particles are heavier and carry more charge as compared to other common nuclear radiation like electrons, protons, neutrons and photons. As a consequence, alpha particles have high linear energy transfer (LET) value and readily give up their energy to the medium through which they pass while disappearing in the process unlike other radiation which may be detected at more convenient distances from the source. Therefore, the online monitoring of alpha radiation from a nuclear facility using conventional detectors presents significant challenges. Semiconducting silicon diodes and metal-oxide semiconductor field effect transistor (MOSFET) dosimeters provide time resolved data[8,9]. Both are very sensitive and provide good resolution but their responses degrade over a finite lifetime. They require power units and data storage and are not amenable for online quantitative estimation. Even though ionization chambers are available nearby, they require a high voltage source and are too large to be employed for online studies[10]. Solid state nuclear track detectors (SSNTD) offer an alternative technique with respect to monitoring alpha particles since they produce atomic displacements and molecular rearrangements along their paths leading to cylindrical shaped trails[11]. Although this technique is simple and sensitive, it involves a time consuming chemical treatment and allows for only off-line monitoring thereby rendering it ineffective during any emergency that requires a prompt response. Instead of enlarging the tracks of alpha radiation with chemical etchant, the authors recently reported that it is possible to correlate the extent of damage of a polymeric solid state nuclear track detector CR-39 film by low level alpha radiation to changes in optical properties like absorbance, reflectance and roughness[12].

Over the past few decades, DNA molecules have developed into an important area of research due to their potential applications in the fields of molecular electronics[13], biosensors[14], computer architectures[15] and massive memories[16]. However, simple forms of DNA molecules such as single strands or duplexes have certain limitations in alignment upon a target substrate with homogeneous distribution and with specific array order thereby causing inconvenience in topology arrangement. DNA nanotechnology serves as useful tools in solving this problem. Self-assembly of programmable Watson-Crick base pairing provides the DNA based building blocks a specific array order resulting in well-ordered DNA crystalline structures. Artificially designed DNA nanostructures are convenient, inexpensive, harmless and amenable for mass production. Additionally, the easy modification utilizing DNA molecules allows DNA nanostructures to enhance functionality by attaching specific proteins, antibodies, dyes or nanoparticles. In the present study we demonstrate its feasibility as a sensitive radiation detector using the

double-crossover (DX) tile based 2D DNA nanostructure[17,18] which has a 0.6 nm single layer thickness in air[19,20]. The analysis of alpha radiation effect of DX tile based DNA thin film on exposure to sub kGray range dose was assessed using atomic force microscopy (AFM) in addition to Raman and reflectance spectroscopic data.

Results

The 2D DNA nanostructure utilized in this study consisted of two repeating DX tiles. A unit DX tile is organized in two DX junctions and two parallel duplexes are tied up. There are two annealing methods for fabrication of DNA nanostructures. While the free-solution method is the commonly used annealing method, substrate-assisted growth (SAG) is also utilized[21–23]. In this study, the SAG method was used to fabricate a DNA thin film over a given substrate due to the limitations of the free-solution method in growing relatively larger DNA crystals in solution[24] and in covering a given substrate completely. Utilizing the SAG method, DNA crystallization including random tile seeding, nucleation and lattice growth was achieved while the annealing process resulted in a polycrystalline DNA thin film with complete coverage controlled by the concentration of DNA molecules[23]. Glass with piranha treatment was used as a substrate. Piranha treated glass (PG) with completely covered polycrystalline DNA nanostructures has distinct advantages due to its transparency which allows for on-line monitoring of changes in DNA structural features on exposure to radiation.

The effect of alpha radiation towards DNA thin film can be controlled by dose (absorbed energy per unit weight of the DNA thin film) which in turn depends on two physical parameters - the distance (d) between the radiation source and the DNA thin film and the radiation exposure time (t_{exp}). Fig. 1 shows an experimental setup and AFM images of the DNA DX lattice (DXL) thin film prior to and following irradiation. Based on the AFM data, we observed that the DXL thin films on PG were gradually deformed and disappeared on exposure to the alpha radiation source, ^{241}Am. An individual DX tile with a dimension of 12 nm × 4 nm is shown in Fig. 1b (inset) as constructed by noise filtered Fourier transform. DNA molecular bonds, especially relatively weak base-to-base hydrogen bonding, can be easily broken when the energy of the alpha particle exceeds DNA base-pairing binding energies. As a result of the exposure to radiation, chemical and hydrogen bonds in the DXL film were broken and the large DXL domain was transformed into smaller crystal domains with increasing radiation doses. AFM data in Fig. 1c and 1d indicate that the radiation effect of d = 2 cm for t_{exp} = 20 min. is relatively more dominant than d = 1 cm for t_{exp} = 10 min. The energy of alpha particles at the ^{241}Am source (5.485 MeV) was attenuated by a 1 cm air column to a peak energy of 4.5 MeV and by a 2 cm air column to a peak energy of 3.5 MeV. The fluence of alpha particles for a 2 cm distance for 20 min. was slightly larger (~1.5 times) than that of a 1 cm distance for 10 min. Since only a fraction of the dose received by the DXL film is absorbed (for details, see Methods in Supplementary Information), the larger damage seen in Fig. 1d as compared to Fig. 1c may be explained on the basis of larger fluence.

The radiation effect on DXL thin films was also studied using Raman spectroscopic analysis to determine the influence of exposure time and the distance of the film from the radiation source (Fig. 2). Without radiation exposure of DXL films show the Raman bands with adenine, cytosine, guanine, thymine bases and phosphate backbone groups with different modes of DNA. The Raman bands observed at 1244 cm^{-1} bending of C-H and stretching of C-N bonds, 1418 cm^{-1} stretching bond in adenine; 655 cm^{-1} stretching mode, 1290 cm^{-1} C-C bond stretching, 1345 cm^{-1} stretching of C-N and

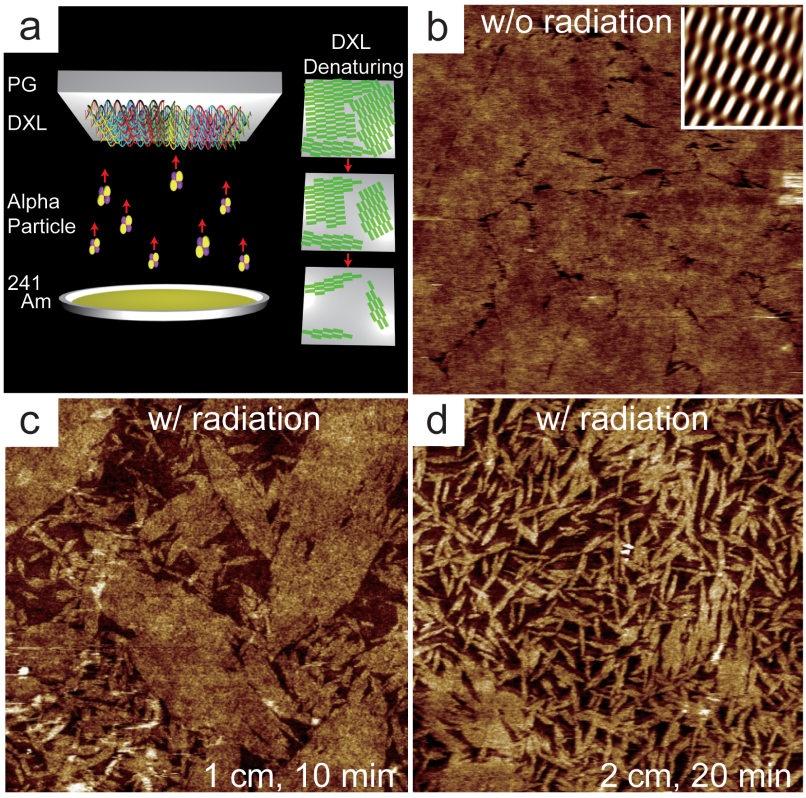

Figure 1 | The alpha particle (^{241}Am) radiation effect on the double crossover lattice (DXL) thin films. (a) Schematic diagram illustrating the alpha particle (^{241}Am) radiation effect on fully covered DXL film on glass substrate. (b – d) AFM images of DXL without and with irradiation. The scan size for all the AFM images are 3 μm × 3 μm unless otherwise noted; (b) without radiation exposure and the insets in top right corner is noise-filtered 2D spectrum image by noise filtered Fourier transform showing the periodicity of the crystals, the scan size is 50 nm × 50 nm. (c) Following radiation exposure from ^{241}Am on DXL film with an exposure distance d = 1 cm and exposure time t_{exp} = 10 min., and (d) for d = 2 cm and t_{exp} = 20 min.

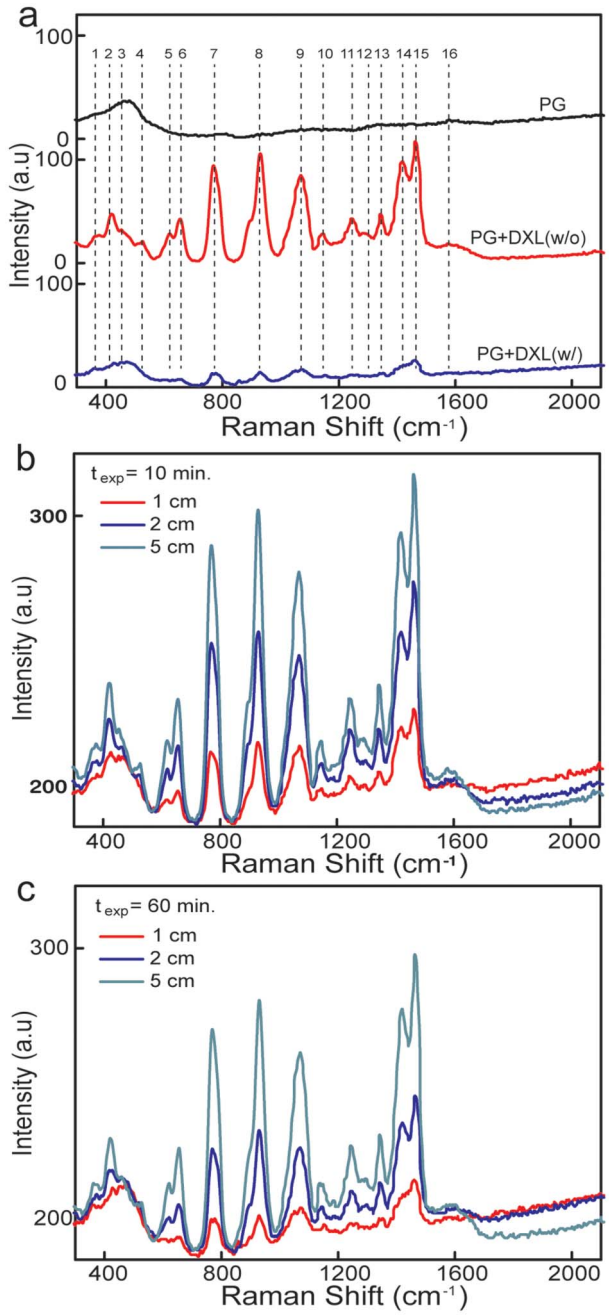

Figure 2 | Comparative Raman spectra without and with radiation exposure on the DXL. (a) PG, PG + DXL without radiation and PG + DXL with radiation exposure at d = 1 cm and t_{exp} of 60 min. (b – c) Radiation exposure effect on the PG + DXL for d = 1, 2 and 5 cm with t_{exp} of 10 min. and 60 min. respectively.

C=C in cytosine; 375 cm^{-1}, 623 cm^{-1} ring stretching, 930 cm^{-1} C-N bond stretching, 1576 cm^{-1} C-N−C=C stretching bonds in guanine; 420 cm^{-1}, 780 cm^{-1} ring breathing mode, 1290 cm^{-1} C-C bond stretching, 1465 cm^{-1} stretching of C-N bonds in thymine; and 530, 1068 cm^{-1} symmetric stretching, 1146 cm^{-1} stretching mode of phosphate backbone. Changes in intensities of selected bands in Raman spectra on radiation exposure of the DXL thin film are summarized in Table 1. The PG, DXL thin film without and with radiation exposure at d = 1 cm and t_{exp} of 60 min. shows the disappearance of a few bands and suppression of the intensities of all other bands corresponding to adenine, thymine, cytosine and guanine constituents of the DXL structure. Otto *et al.* measured

Table 1 | Assignment of Raman bands of double crossover lattice (DXL) DNA thin film and corresponding intensity changes at d = 1 cm, t_{exp} = 60 min. after alpha radiation

Serial pick no.	Band positions before exposure (cm^{-1})	Intensity changes following exposure (%)	Bond assignment
1	375	39	Guanine
2	420	52	Thymine
3	475	39	Glass
4	530	100	Phosphate backbone
5	623	100	Ring stretching mode in Guanine
6	655	83	Stretching mode in Cytosine
7	780	86	Ring breathing mode in Thymine
8	930	86	C-N bond stretching in Guanine
9	1068	79	Symmetric stretching of phosphate backbone
10	1146	60	Phosphate backbone
11	1244	73	Bending of C-H and stretching of C-N bonds in Adenine
12	1290	53	C-C bond stretching in Cytosine, Thymine
13	1345	100	Stretching of C-N and C=C bond in Cytosine
14	1418	100	Adenine
15	1465	78	Stretching of C-N bond in Thymine
16	1576	100	Stretching of C-N−C=C bonds in Guanine

the surface enhanced Raman spectral peaks for each DNA base and Vasudev *et al.* explained the vibrational modes of DNA molecules immobilized on substrates[25,26]. The band assignments depicted in the Raman spectra in our report are in accordance with previous studies[25–28].

The exposure effects on DXL thin films for d = 1, 2 and 5 cm with t_{exp} of 10 min. and 60 min. were also measured (Fig. 2b and 2c). The Raman bands of DXL film for t_{exp} of 10 min. and d = 5 cm show bands similar to the unexposed DXL but at t_{exp} = 10 min. and d = 1 cm, two bands (at 530, 1576 cm^{-1}) disappeared. The Raman bands at d = 1 cm and t_{exp} = 60 min. resulted in the disappearance of three additional bands (623, 1345 and 1418 cm^{-1}) with significantly reduced intensities for the remaining bands. This is a consequence of the structural damage caused by the absorbed alpha radiation dose. The peak intensities gradually increased with increasing distance from the ^{241}Am radiation source as the dose due to the alpha radiation decreased significantly with distance. Thus, the absorbed dose and the damage caused to the DXL thin film were proportionately reduced at increasing distances. In contrast, the radiation effect around 5 cm was negligible since the range of alpha particles in the air is less than 5 cm. Consequently, the Raman shifts and intensities of Raman bands at 5 cm were similar to those of unirradiated DXL. Based on the Raman spectral analysis, deformation of DNA lattices was unambiguous at a distance of 1 and 2 cm from the source, even for a radiation exposure time of 10 min.

The schematic of the fiber optic reflectance probe employed for the optical evaluation of the DXL thin film on exposure to ^{241}Am alpha source is depicted in Fig. 3. The ray diagram (upper left corner of Fig. 3a) illustrates the multiple reflections occurring from the PG and DXL thin film. When the incident light interacts with the DXL thin film, a fraction of the light is reflected from the surface while another fraction is absorbed and the remainder is transmitted through the surface. The reflected light from the PG surface as well as the light

passing through the DXL thin film was measured by a spectrometer and photo detector. The reflected intensities of glass and PG without the DXL thin film were very similar as shown in Fig. 3b. The reflected intensities of air without any glass, PG and DXL showed less intensity. The reflected intensity with the DXL thin film recorded online during exposure to ^{241}Am for an hour, with varying distances of the source from the DXL thin film (from 1 to 5 cm) is shown in Fig. 3c. The change in the reflected intensity, as measured by the spectrometer, was similar for irradiation distances of 1 and 2 cm. However, for a 5 cm irradiation distance, the change in reflected intensity was reduced significantly since the mean range of alpha particles in the air is about 3.5 cm. Therefore, the fluence of alpha particles dramatically declines near the 5 cm irradiation distance. Fig. 3d shows the reflected intensity, as measured by the photo detector, for an irradiation distance of 1 cm over a period of 15 min. The change in reflected light was observed to be 2.2 mV which was significantly larger than that of PG, 0.5 mV. Based on our observations, it would seem plausible to set an alarm signal which could be activated remotely once a defined threshold reflectance intensity change occurs.

Discussion

The radiation source in the present work, ^{241}Am, emits alpha particles ($331s^{-1}$ in 2π steradian) with initial energies of 5.485 MeV (85%), 5.443 MeV (13%) and 5.388 MeV (2%). The principle photon emitted has an energy of 59.5 keV with a yield of around 36%. In view of the much larger LET value of alpha particles as compared to photons, the latter is neglected in the present discussion. Furthermore, since the three emitted alpha particles are very close in energy, we considered the particle with a mean energy of 5.48 MeV. In air, this value decreases to 4.5 MeV at a distance of 1 cm and to 3.5 MeV at a distance of 2 cm. It has a range of about 3.5 cm in air[29]. It appears that the dose absorbed though a miniscule small fraction of the total dose required to rupture chemical/hydrogen bonds of DXL samples (refer to Methods in Supplementary Information), is sufficient to cause the damage seen in Fig. 1 and Fig. 2. The damage caused is proportionate to the dose absorbed which varies with time and distance. Raman and reflectance spectroscopy data suggest that the dose absorbed in 10 min. at a distance of 1 and 2 cm is sufficient in revealing topological differences in the DXL thin film.

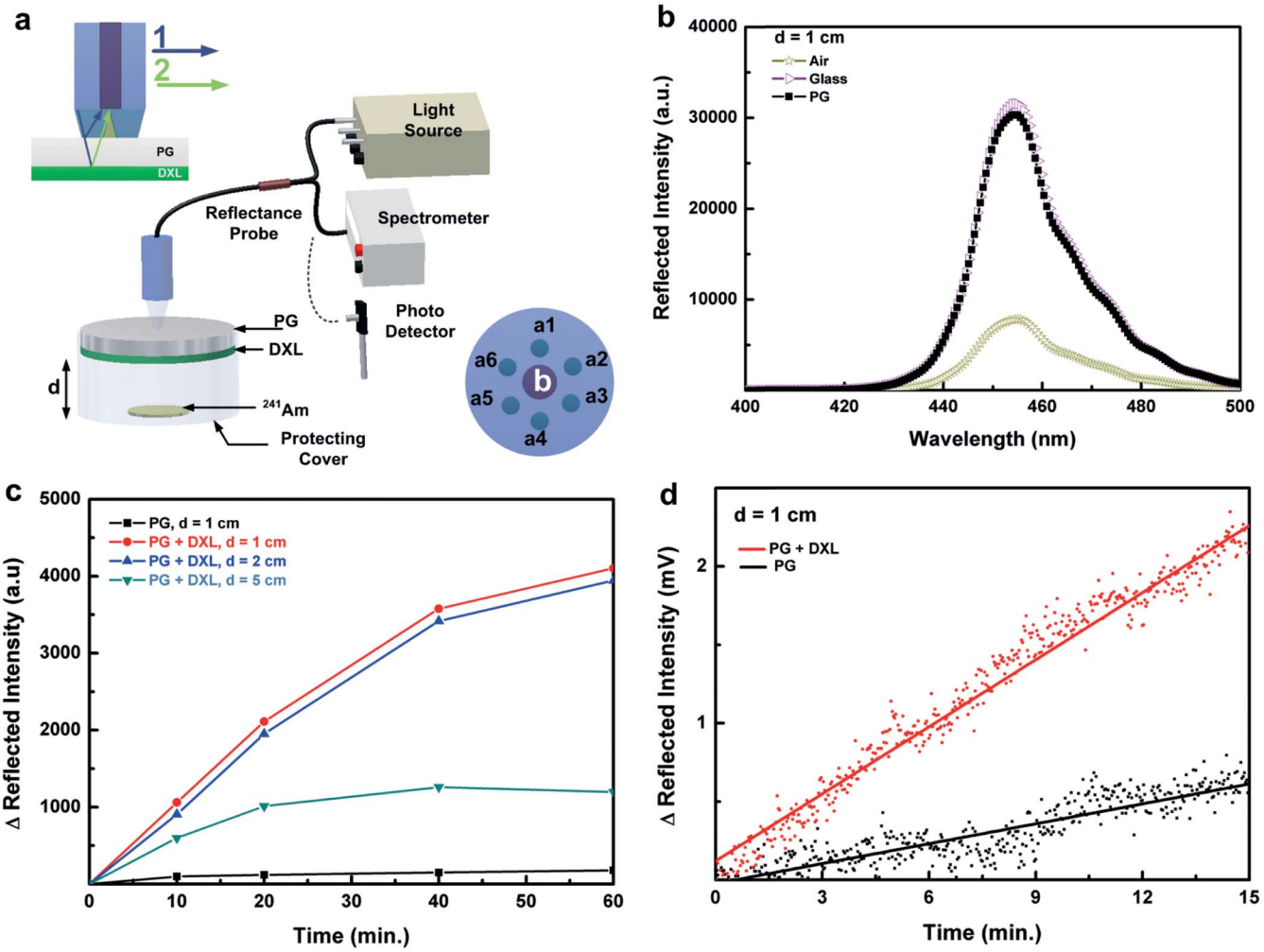

Figure 3 | Optical characteristics of the DXL upon radiation exposure. (a) Schematic diagram illustrating the experimental setup used for the evaluation of optical characteristics of the DXL upon exposure to radiation from ^{241}Am alpha particle source. The reflectance probe was placed at a fixed distance of 1 cm from PG and the reflected light signal was measured using a spectrometer and silicon photo detector. The reflectance probe tip consisted of six illuminating fibers (a1 to a6) and one reflected light fiber at the center (b) as shown in right bottom corner. The ray diagram of incident light and reflected light from PG and the DXL is shown in the upper left corner where 1 (blue arrow) corresponds to incident light and reflected light from the top of PG and 2 (green) corresponds to the reflected light from the bottom surface of PG and the DXL film. (b) The reference spectrograph for air, glass and PG. (c) The change in reflected light intensity controlled by exposure time at various distances d = 1, 2, and 5 cm. The experimental error is estimated to be within ±5%. (d) The change in reflected light intensity as measured by silicon photo detector at d = 1 cm for t_{exp} up to 15 min.

In conclusion, the present work shows that the changes observed in synthesized DNA thin film on exposure to alpha particles in air for a few min. are significant with respect to the topological changes observed by AFM, Raman spectrum and optical reflectance intensity changes as measured by a photo detector, on-line photo spectroscopy. Specifically, this is due to the fact that the available energy within a single alpha particle, 7.2×10^{-13} J, is sufficient in damaging 1.2×10^5 DXL units since the energy of hydrogen bonds in one DXL unit is 6.1×10^{-18} J. Considering that the radiation source contained only 6 ng of ^{241}Am, changes in reflectance intensity of 1 mV on exposure of the DXL thin film for 6 min. at a distance of 1 cm suggests that the thin film could form the basis of an ultra-sensitive alpha detector by further decreasing the distance thereby increasing the sensitivity of the reflectance probe. Fabrication of efficient sensors constructed using biomolecules is one of the major research areas in bionanotechnology and will provide a novel platform in constructing devices and sensors with high reliability in the future.

Methods

Substrate assisted growth process. The glass substrate with a size of 0.3×0.3 cm^2 was cleaned with piranha solution (H_2O_2 (30%) : H_2SO_4 (96%) = 1 : 2) for 30 min., followed by rinses with deionized water. Subsequently, the substrates were incubated in a physiological buffer, $1 \times$ TAE/Mg^{2+} buffer solution, for deprotonation. The piranha treated glass (PG) substrate was then utilized in a SAG annealing process. Synthetic oligonucleotides, purified by HPLC, were purchased from Integrated DNA Technologies (IDT, Coralville, IA). Complexes were formed by mixing a stoichiometric quantity of each strand in the $1 \times$ TAE/Mg^{2+}. A final concentration of 70 nM was achieved. For annealing, the PG along with the DNA strands were inserted into an AXYGEN tube which was then placed in a Styrofoam box with 2 L of boiled water and subsequently cooled from 95 °C to 25 °C gradually over a period of at least 24 hours in order to facilitate the hybridization process.

Alpha particle source. The radionuclide ^{241}Am was used as the source of alpha particles. This radionuclide was chosen due to its long physical half-life (432.2 years) and widespread availability owing to its use in smoke detection systems and for industrial gauging applications. The principal alpha particle radiation emissions were 5.485, 5.443 and 5.388 MeV with corresponding yields per decay of 0.845, 0.13 and 0.016, respectively. The source strength was 729 Bq. The alpha surface emission rate was 331 s^{-1} in 2π steradian. ^{241}Am was incorporated into the surface of an anodized Al foil of 0.3 mm thickness. The thickness of the active layer was 6 μm and the diameter of the active surface was 58 mm.

AFM imaging and Raman spectra. For AFM imaging, a substrate assisted grown sample was placed on a metal puck using instant glue. 30 μL $1 \times$ TAE/Mg^{2+} buffer was added onto the substrate and another 10 μL of $1 \times$ TAE/Mg^{2+} buffer was dispensed into the AFM tip (Veeco Inc.). AFM images were obtained with a Multimode Nanoscope (Veeco Inc.) in the liquid tapping mode. Before measuring the Raman spectra, the samples are rinsed with deionized water, followed by fine blowing with nitrogen gas for removing chemical residues from the DXL thin film on a PG substrate. The measurements were performed at room temperature with the confocal Raman microscope (WITec, alpha 300 R) at 532 nm.

Reflectance measurement. A reflectance probe (R600-8 UV-VIS SR, StellarNet Inc, USA) with 7 optical fibers bundled around 1600 μm fiber was utilized. For reflectance measurements, the 6 exterior fibers were illuminated by a light source (λ = 460 nm, WT&T Inc., USA) and the interior fiber collected the reflected light and returned the signal to the spectrometer (AvaSepc-2048, USA) and the photo detector (PDA36A-EC, Thorlab, USA).

1. Clery, D. Current Designs Address Safety Problems in Fukushima Reactors. *Science* **331**, 1506 (2011).
2. Kintisch, E. Japan disaster. Pool at stricken reactor #4 holds answers to key safety questions. *Science* **332**, 24–25 (2011).
3. Brumfiel, G. How a handful of operators at a crippled reactor averted a greater catastrophe at the Fukushima plant. *Nature* **471**, 417–418 (2011).
4. Stone, R. Fukushima Cleanup Will Be Drawn Out and Costly. *Science* **331**, 1507 (2011).
5. Butler, D. Fukushima health risks scrutinized. *Nature* **472**, 13–14 (2011).
6. Brumfiel, G. Japan's long road ahead. *Nature* **472**, 14 (2011).
7. Kaiser, J. Radiation Risks Outlined by Bombs, Weapons Work, and Accidents. *Science* **331**, 1504 (2011).
8. Ehringfeld, C. *et al.* Application of commercial MOSFET detectors for in vivo dosimetry in the therapeutic x-ray range from 80 kV to 250 kV. *Phys. Med. Biol.* **50**, 289–303 (2005).
9. Jornet, N. *et al.* Comparison study of MOSFET detectors and diodes for entrance in vivo dosimetry in 18 MV x-ray beams. *Med. Phys.* **31**, 2534–2542 (2004).
10. Huq, M. S. & Andreo, P. Advances in the determination of absorbed dose to water in clinical high-energy photon and electron beams using ionization chambers. *Phys. Med. Biol.* **49**, R49–R104 (2004).
11. Fleischkr, R. L., Price, P. B. & Walker, R. M. Track Registration in Various Solid-State Nuclear Track Detectors. *Phys. Rev.* **133**, 1443–1449 (1964).
12. Kulkarni, A. *et al.* Online optical monitor of alpha radiations using a polymeric solid state nuclear track detector CR-39. *Sensors and Actuators B* **161**, 697–701 (2012).
13. Genereux, J. C. & Barton, J. K. Molecular Electronics: DNA Charges Ahead. *Nature Chemistry* **1**, 106–107 (2009).
14. Wang, J., Jiang, M., Nilsen, T. W. & Getts, R. C. Dendritic Nucleic Acid Probes for DNA Biosensors. *J. Am. Chem. Soc.* **120**, 8281–8282 (1998).
15. Benenson, Y. *et al.* Programmable and autonomous computing machine made of biomolecules. *Nature* **414**, 430–343 (2001).
16. Calude, C. S. & Casti, J. L. Computing: Parallel thinking. *Nature* **392**, 549–551 (1998).
17. Fu, T. J. & Seeman, N. C. DNA double crossover molecules. *Biochemistry* **32**, 3211–3220 (1993).
18. Winfree, E., Liu, F., Wenzler, L. A. & Seeman, N. C. Design and self-assembly of two-dimensional DNA crystals. *Nature* **394**, 539–544 (1998).
19. Park, S. H., Prior, M. W., LaBean, T. H. & Finkelstein, G. Optimized fabrication and electrical analysis of silver nanowires templated on DNA molecules. *Appl. Phys.Lett.* **89**, 033901–3 (2006).
20. Moreno-Herrero, F.,Colchero, J. & Baro, A. M. DNA height in scanning force microscopy. *Ultramicroscopy* **96**, 167–174 (2003).
21. Hamada, S. & Murata, S. Substrate-assisted assembly of interconnected single-duplex DNA nanostructures. *Angew.Chem. Int. Ed.* **48**, 6820–6823 (2009).
22. Kim, B., Amin, R., Lee, J., Yun, K. & Park, S. H. Growth and restoration of a T-tile-based 1D DNA nanotrack. *Chem. Commun.* **47**, 11053–11055 (2011).
23. Lee, L. *et al.* Coverage Control of DNA Crystals Grown by Silica Assistance. *Angew.Chem. Int. Ed.* **50**, 9145–9149 (2011).
24. Liu, H., He, Y., Ribbe, A. E. & Mao, C. Two-Dimensional (2D) DNA Crystals Assembled from Two DNA Strands. *Biomacromolecules* **6**, 2943–2945 (2005).
25. Otto, C., van den Tweel, T. J. J., De Mu1, F. F. M. & Greve, J. Surface-Enhanced Raman Spectroscopy of DNA Bases. *J. Raman Spectrosc.* **17**, 289–298 (1986).
26. Vasudev, M. *et al.* Optoelectronic signatures of DNA-based hybrid nanostructures. *IEEE Transaction on nanotechnology* **10**, 35–43 (2011).
27. Ponkumar, S., Duraisamy, P. & Iyandurai, N. Structural Analysis of DNA Interactions with Magnesium Ion Studied by Raman Spectroscopy. *Am. J. Bioche. & Biotech.* **7**, 135–140 (2011).
28. Cristina, M., Muntean, R. M., Lubomir, D. & Heinz, W. Mn^{2+}–DNA Interactions in Aqueous Systems: A Raman Spectroscopic Study. *Spectroscopy* **20**, 29–35 (2006).
29. Yu, K. N., Yip, C. W. Y.,Nikezic, D., Ho, J. P. Y. & Koo, V. S. Y. Comparison among alpha-particle energy losses in air obtained from data of SRIM, ICRU and experiments. *Appl.Radiat. Isot.* **59**, 363–366 (2003).

Acknowledgements

This research was supported by the National Research Foundation of Korea (NRF) grant (R31-2008-10029, WCU program) to V.M., (2009-0083540, BSR Program), (S-2011-1039-007-1, GRRC program) to T.K. and (2010-0013294, BSR Program), (2012R1A6A1040282, PRC Program) to S.H.P. funded by the Korea government (MEST).

Author contributions

A.K., D.S.R. and B.H.K. conceived and initiated this project. D.S.R. prepared the samples, D.S.R., A.K., B.H.K., J.A.K. and P.J. preformed AFM, Raman, Optical measurements and collected the data. D.S.R. and J.A.K. carried out the control experiment with UV source. All authors contributed to the data analysis. A.K., D.S.R. and B.H.K. wrote the manuscript with contributions from V.M., T.K. and S.H.P., V.M., T.K. and S.H.P. supervised this research.

Additional information

Supplementary information accompanies this paper at http://www.nature.com/scientificreports

Competing financial interests: The authors declare no competing financial interests.

How to cite this article: Kulkarni, A. *et al.* A novel nanometric DNA thin film as a sensor for alpha radiation. *Sci. Rep.* **3**, 2062; DOI:10.1038/srep02062 (2013).